Cyclometallated ruthenium(III) complexes: Synthesis, structure and properties

Raji Raveendran, Samudranil Pal *

School of Chemistry, University of Hyderabad, Hyderabad 500 046, India

ARTICLE INFO

ABSTRACT

Reactions of Schiff bases (H$_2$apahR) derived from acetophenone and acid hydrazides, triethylamine and [Ru(PPh$_3$)$_3$Cl$_2$] (1:2:1 mole ratio) in methanol provide cyclometallated ruthenium(III) complexes of formula trans-[Ru(apahR)(PPh$_3$)$_2$Cl] in 74–81% yields. The complexes have been characterized by elemental analysis, magnetic susceptibility, spectroscopic (infrared, electronic and EPR) and electrochemical measurements. X-ray crystal structures of two representative complexes have been determined. In each complex, the metal centre is in distorted octahedral CNOClP$_2$ coordination sphere assembled by the C,N,O-donor meridionally spanning apahR^{2-}, the chloride and the two mutually trans-oriented PPh$_3$ molecules. All the complexes are one-electron paramagnetic ($\mu_{eff.}$ = 1.85–1.98 μ_B) and display rhombic EPR spectra in frozen (120 K) dichloromethane-toluene (1:1) solution. Electronic spectra of the complexes display several absorptions within 470–270 nm due to ligand-to-metal charge transfer and ligand centred transitions. The complexes are redox active and display a Ru(III) → Ru(II) reduction and a Ru(III) → Ru(IV) oxidation in the potential ranges −0.66 to −0.70 V and 0.75 to 0.80 V (vs. Ag/AgCl), respectively.

© 2009 Elsevier B.V. All rights reserved.

1. Introduction

Organometallic chemistry of ruthenium is dominated primarily by its diamagnetic +2 oxidation state [1–3]. Authentic ruthenium(III) species having M–C σ-bond are very rare [4–15]. A handful of these ruthenium(III) complexes belong to the cyclometallated type of species [11–14]. Among these very few cyclometallated complexes, only one is X-ray structurally characterized [11]. We have been working on cyclopalladated complexes with C,N,O-donor acid hydrazide based Schiff bases during the last few years [15,16]. Recently we have reported a series of trans-chlorobis(triphenylphosphine)ruthenium(III) complexes with the same class of C,N,O-donor Schiff bases derived from benzaldehyde and various acid hydrazides [17]. These one-electron paramagnetic and EPR active complexes display a Ru(III) → Ru(IV) oxidation in the cyclic voltammetry. This observation indicates that, this ligand system is not only able to stabilize cyclometallated ruthenium(III) but also makes ruthenium(IV) accessible. Using the analogous Schiff bases (H$_2$apahR) prepared from acetophenone and acid hydrazides we have prepared a new series of cyclometallated ruthenium(III) complexes and compared their physical properties with our previously reported complexes [17]. In the following account, we describe the synthesis, characterization and properties of the complexes, trans-[Ru(apahR)(PPh$_3$)$_2$Cl]. X-ray structures of two representative complexes are also reported.
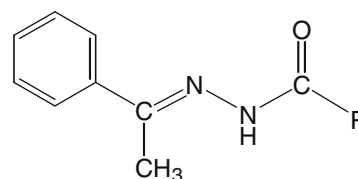
H$_2$apahR
R = CH$_3$, C$_6$H$_5$, 4-CH$_3$-C$_6$H$_4$,
4-H$_3$CO-C$_6$H$_4$, 4-Cl-C$_6$H$_4$

2. Experimental

2.1. Materials

The Schiff bases H$_2$apahR were prepared in ∼80% yields by condensation reactions of one mole equivalent of acetophenone with one mole equivalent of the corresponding acid hydrazide in methanol. [Ru(PPh$_3$)$_3$Cl$_2$] was prepared by following a reported procedure [18]. All other chemicals and solvents were of analytical grade available commercially and were used as received.

2.2. Physical measurements

Elemental (C, H, N) analysis data were obtained with a Thermo Finnigon Flash EA1112 series elemental analyzer. Room

temperature (298 K) magnetic susceptibilities were measured using a Sherwood Scientific balance. Diamagnetic corrections calculated from Pascal's constants [19] were used to obtain the molar paramagnetic susceptibilities. Solution electrical conductivities were measured with a Digisun DI-909 conductivity meter. Infrared spectra were collected by using KBr pellets on a Nicolet 5700 FT-IR spectrophotometer. A Cary 100 Bio UV/vis spectrophotometer was used to record the electronic spectra. EPR spectra were recorded on a Jeol JES-FA200 spectrometer. A CH-Instruments model 620A electrochemical analyzer was used for cyclic voltammetric experiments with dimethylformamide solutions of the complexes containing tetrabutylammonium perchlorate (TBAP) as the supporting electrolyte. The three electrode measurements were carried out at 298 K under dinitrogen atmosphere with a platinum disk working electrode, a platinum wire auxiliary electrode and an Ag/AgCl reference electrode. Under identical condition the Fc^+/Fc couple was observed at 0.54 V. The potentials reported in this work are uncorrected for junction contributions.

2.3. Synthesis of $[Ru(apahCH_3)(PPh_3)_2Cl]$ (1)

Solid $[Ru(PPh_3)_3Cl_2]$ (270 mg, 0.28 mmol) was added to a yellow methanol solution (30 ml) of $H_2apahCH_3$ (50 mg, 0.28 mmol) and $N(C_2H_5)_3$ (0.08 ml, 58 mg, 0.57 mmol) and the mixture was boiled under reflux for 2 h. On cooling to room temperature the complex was precipitated from the reaction mixture as a light brown solid. It was collected by filtration, washed thoroughly with hexane and dried in air. This solid was dissolved in minimum amount of dichloromethane and transferred to a neutral aluminium oxide column. The first moving light yellow band containing the unreacted ligand was eluted with dichloromethane and discarded. The second brown band containing the complex was eluted with dichloromethane containing 5% acetone. Recrystallization of the complex was performed from dichloromethane-hexane (1:1) mixture. Yield, 190 mg (81%).

The other four complexes having the same general formula trans-$[Ru(apahR)(PPh_3)_2Cl]$ (2 (R = C_6H_5), 3 (R = 4-CH_3–C_6H_4), 4 (R = 4-CH_3O–C_6H_4) and 5 (R = 4-Cl–C_6H_4)) reported in this work were synthesized from $[Ru(PPh_3)_3Cl_2]$, the corresponding Schiff base (H_2apahR) and $N(C_2H_5)_3$ (1:1:2 mole ratio) in 74–80% yields by following procedures very similar to that described above for 1 (R = CH_3).

2.4. X-ray crystallography

The single crystals of 1 and 5 were grown by slow evaporation of their solutions in dichloromethane-hexane (1:1) mixture. Unit cell parameters and the intensity data for both 1 and 5 were obtained on a Bruker–Nonius SMART APEX CCD single crystal diffractometer, equipped with a graphite monochromator and a Mo Kα fine-focus sealed tube (λ = 0.71073 Å) operated at 2.0 kW. The detector was placed at a distance of 6.0 cm from the crystal and the data were collected at 298 K with a scan width of 0.3° in ω and an exposure time of 15 s/frame. The SMART software was used for data acquisition and the SAINT-Plus software was used for data extraction [20]. The data were corrected for absorption with the help of SADABS program [21]. Complexes 1 and 5 crystallize in the space groups $P2_1/c$ and $P\bar{1}$, respectively. The structures were solved by direct methods and refined on F^2 by full-matrix least-squares procedures. In each case, the asymmetric unit contains one complete complex molecule. For both 1 and 5, the chlorine atom is disordered in two positions. It has been refined with half occupancy at each position. All non-hydrogen atoms were refined anisotropically. The hydrogen atoms were included in the structure factor calculation at idealized positions by using a riding model. The SHELX-97 programs [22] were used for structure solution and

Table 1
Crystal data for trans-$[Ru(apahCH_3)(PPh_3)_2Cl]$ (1) and trans-$[Ru(apah4-Cl-C_6H_4)-(PPh_3)_2Cl]$ (5).

Complex	1	5
Chemical formula	$RuC_{46}H_{40}N_2OClP_2$	$RuC_{51}H_{41}N_2OCl_2P_2$
Formula weight	835.26	931.77
Crystal system	Monoclinic	Triclinic
Space group	$P2_1/c$	$P\bar{1}$
a (Å)	9.9071(12)	10.693(3)
b (Å)	19.192(2)	10.718(3)
c (Å)	20.429(2)	20.654(6)
α (°)	90	97.974(4)
β (°)	92.441(2)	101.662(4)
γ (°)	90	109.545(4)
V (Å³)	3880.9(8)	2129.3(1)
Z	4	2
ρ (g cm⁻³)	1.430	1.453
μ (mm⁻¹)	0.594	0.611
Reflections collected	39901	21820
Reflections unique	7664	8244
Reflections $[I \geqslant 2\sigma(I)]$	6854	7393
Parameters	489	542
R_1, wR_2 $[I \geqslant 2\sigma(I)]$	0.0330, 0.0837	0.0330, 0.0769
R_1, wR_2 [all data]	0.0378, 0.0867	0.0378, 0.0792
GOF on F^2	1.034	1.031
Largest peak and hole (e Å⁻³)	0.681, −0.610	0.428, −0.321

refinement. The ORTEX6a package [23] was used for molecular graphics. Selected crystal data are listed in Table 1.

3. Results and discussion

3.1. Synthesis and some properties

Reactions of $[Ru(PPh_3)_3Cl_2]$, corresponding H_2apahR and $N(C_2H_5)_3$ (1:1:2 mole ratio) in methanol under aerobic condition provide the complexes 1–5 in very good yields. Elemental analysis data (Table 2) for the complexes are consistent with the general molecular formula $[Ru(apahR)(PPh_3)_2Cl]$. The complexes are brown in color and electrically nonconducting in solutions. The room temperature (298 K) effective magnetic moments measured with powdered samples of 1–5 are in the range 1.88–1.98 μ_B (Table 2). These values confirm the +3 oxidation state and the low-spin character of the metal centre in each complex.

3.2. Spectroscopic characteristics

Absence of the characteristic bands associated with the N–H and C=O bonds of the amide functionality [24,25] in the infrared spectra of 1–5 indicates its enolate form in the metal bound tridentate ligand. The medium to strong band observed within 1609–1574 cm⁻¹ is attributed to the C=N—N=C fragment of $apahR^{2-}$. Three strong bands observed at ~744, ~693 and ~515 cm⁻¹ are consistent with the presence of trans-$\{Ru(PPh_3)_2\}$ unit in all the complexes [13,17,26–29].

Electronic spectra of 1–5 were recorded with their dichloromethane solutions. The data are listed in Table 2. The spectral profiles of 1–5 are not very different from that of our previously reported analogous complexes with the acid hydrazide based Schiff bases derived from benzaldehyde [17]. There are two moderately intense absorptions in the wavelength range 470–350 nm for all the complexes. These are very likely to be due to the ligand-to-metal charge transfer transitions expected for low-spin ruthenium(III) complexes [11–14,17,26,28,29,31]. In the UV region, the very intense band displayed by all the complexes within the wavelength range 277–270 nm and the preceding shoulder observed for some of the complexes are believed to be due to ligand based transitions.

In frozen (120 K) dichloromethane-toluene (1:1) solution, the EPR spectra of all the complexes are very similar and display three

Table 2
Elemental analysis, electronic spectroscopic and magnetic susceptibility data.
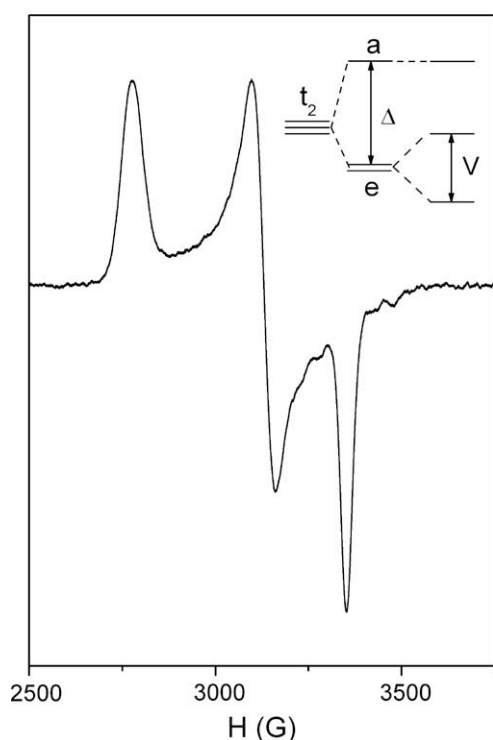
Complex	Found (Calc.) (%)			λ_{max} (nm) ($10^{-3} \times \varepsilon$ (M^{-1} cm^{-1}))[a]	$\mu_{eff.}$ (μ_B)[b]
	C	H	N		
1	65.98 (66.14)	4.65 (4.83)	3.13 (3.35)	450 (0.86), 350[c] (3.7), 275 (29.4)	1.91
2	68.05 (68.26)	4.60 (4.72)	3.02 (3.12)	460 (1.9), 385[c] (3.0), 340[c] (6.7), 270 (27.4)	1.88
3	68.21 (68.52)	4.56 (4.87)	2.88 (3.07)	465 (2.5), 387[c] (5.1), 328[c] (10.8), 277 (37.7)	1.90
4	67.17 (67.35)	4.63 (4.78)	2.95 (3.02)	450 (3.5), 370[c] (6.5), 270 (37.3)	1.96
5	65.53 (65.74)	4.29 (4.43)	2.89 (3.01)	470 (2.3), 390[c] (3.7), 345[c] (9.3), 275 (41.5)	1.98

[a] In dichloromethane.
[b] At 298 K.
[c] Shoulder.

distinct signals. The EPR data are listed in Table 3 and a representative spectrum is shown in Fig. 1. Such rhombic spectra are typical for low-spin ruthenium(III) species having distorted octahedral coordination geometry. The axial (Δ) and the rhombic (V) components of this distortion have been calculated from the EPR g-values using the g tensor theory for low-spin d^5 metal ion complexes [30]. The axial component splits the t_2 level into "a" and "e" levels and the rhombic component removes the degeneracy of "e" level (Fig. 1). The energies of these levels are also affected by the

spin–orbit coupling. Therefore within these three levels two ligand-field transitions of energies ΔE_1 and ΔE_2 ($\Delta E_1 < \Delta E_2$) are possible. The distortion parameters and the transition energies are summarized in Table 3. The ΔE_1 and ΔE_2 transitions for **1–5** are expected to occur in the ranges 5565–6160 cm^{-1} (1797–1623 nm) and 15545–19407 cm^{-1} (643–515 nm), respectively. The Δ/V ratios for **1–5** are in the range 0.95–1.07. It may be noted that the Δ/V ratios are within 1.01–1.16 for our previously reported analogues complexes [17]. Thus the rhombic component of the distortion is somewhat more dominant in the present series of complexes. This increase in the rhombicity may be due to the replacement of the —CH=N— moiety present in the previously reported complexes by the relatively more bulky —C(CH₃)=N— moiety in the present series of complexes.

3.3. X-ray structures of *1* and *5*

The molecular structures of **1** and **5** are illustrated in Figs. 2 and 3, respectively. Structural parameters associated with the metal ion for both complexes are listed in Table 4. In each complex, the metal centre is in distorted octahedral $CNOClP_2$ coordination sphere. The tridentate dianionic C,N,O-donor ligand binds the metal centre in a meridional fashion and forms two five-membered chelate rings. The two phosphine ligands are in mutually *trans* positions. The disordered Cl-atom satisfies the remaining equatorial position. For clarity only one of the two half occupancy Cl-atoms are shown in Figs. 2 and 3. The bond lengths in the tridentate ligands are unexceptional and indicate the enolate form

Table 3
EPR g-values,[a] distortion parameters and near-IR transitions[b].

| Complex	g_1	g_2	g_3	Δ/λ	V/λ	$\Delta E_1/\lambda$	$\Delta E_2/\lambda$
1	2.33	2.09	1.95	10.703	−10.351	5.616	15.981
2	2.36	2.09	1.95	11.089	−11.629	5.565	17.201
3	2.34	2.10	1.95	10.527	−9.831	5.698	15.545
4	2.35	2.09	1.95	11.094	−11.206	5.581	16.796
5	2.32	2.08	1.96	12.699	−13.241	6.160	19.407

[a] In 1:1 dichloromethane–toluene at 120 K.
[b] The calculations are based on the spin–orbit coupling constant (λ) = 1000 cm^{-1}.

Fig. 1. X-band EPR spectrum of *trans*-[Ru(apahC₆H₅)(PPh₃)₂Cl] (**2**) in frozen (120 K) dichloromethane-toluene (1:1) solution and the t_2 splitting pattern.

Fig. 2. Molecular structure of *trans*-[Ru(apahCH₃)(PPh₃)₂Cl] (**1**) with the atom labeling scheme. All atoms are represented by their 30% probability thermal ellipsoids. Hydrogen atoms are omitted for clarity.
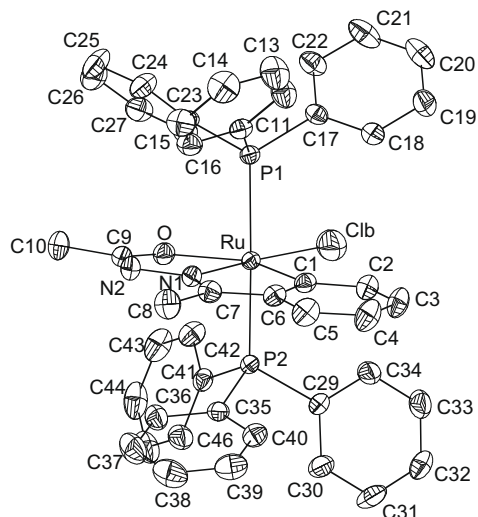
Fig. 3. Molecular structure of *trans*-[Ru(apah4-Cl-C₆H₄)(PPh₃)₂Cl] (**5**) with the atom labeling scheme. All atoms are represented by their 30% probability thermal ellipsoids. Hydrogen atoms are omitted for clarity.

of the amide functionality in both complexes. The chelate rings formed by the tridentate ligand are satisfactorily planar in both complexes. The mean deviations are in the range 0.002–0.04 Å. The two rings are also essentially coplanar in each complex. The dihedral angles between the two ring planes are 3.6(1)° and 3.7(1)° for **1** and **5**, respectively. The bite angle (73.59(7)° for **1** and 74.24(6)° for **5**) in the chelate ring formed by the amide-O and the imine-N is slightly smaller than that (75.85(9)° for **1** and 75.38(8)° for **5**) in the chelate ring formed by the imine-N and the ring-C. The P1–Ru–P2 angles (175.51(2)° for **1** and 174.51(2)°

Table 4
Selected structural parameters (lengths (Å) and angles (°)) for *trans*-[Ru(apahCH₃)(PPh₃)₂Cl] (**1**) and *trans*-[Ru(apah4-Cl-C₆H₄)(PPh₃)₂Cl] (**5**).

1[a]		**5**[b]	
Ru–O	2.1085(17)	Ru–O	2.1164(16)
Ru–N(1)	2.0580(19)	Ru–N(1)	2.0464(18)
Ru–C(1)	2.066(2)	Ru–C(1)	2.068(2)
Ru–P(1)	2.3969(6)	Ru–P(1)	2.4226(7)
Ru–P(2)	2.3924(6)	Ru–P(2)	2.3783(7)
Ru–Cl(a)	2.1179(16)	Ru–Cl(1a)	2.0038(15)
Ru–Cl(b)	2.019(2)	Ru–Cl(1b)	2.0026(16)
O–Ru–N(1)	73.59(7)	O–Ru–N(1)	74.24(6)
O–Ru–C(1)	149.13(9)	O–Ru–C(1)	149.33(8)
O–Ru–P(1)	89.71(5)	O–Ru–P(1)	88.87(5)
O–Ru–P(2)	87.51(5)	O–Ru–P(2)	93.30(5)
N(1)–Ru–C(1)	75.85(9)	N(1)–Ru–C(1)	75.38(8)
N(1)–Ru–P(1)	90.70(6)	N(1)–Ru–P(1)	92.05(5)
N(1)–Ru–P(2)	91.89(6)	N(1)–Ru–P(2)	93.62(6)
C(1)–Ru–P(1)	94.98(7)	C(1)–Ru–P(1)	96.33(6)
C(1)–Ru–P(2)	89.21(7)	C(1)–Ru–P(2)	84.49(6)
P(1)–Ru–P(2)	175.51(2)	P(1)–Ru–P(2)	174.28(2)
O–Ru–Cl(a)	92.99(7)	O–Ru–Cl(1a)	88.42(6)
O–Ru–Cl(b)	129.50(8)	O–Ru–Cl(1b)	128.00(6)
N(1)–Ru–Cl(a)	166.43(8)	N(1)–Ru–Cl(1a)	162.64(7)
N(1)–Ru–Cl(b)	156.49(9)	N(1)–Ru–Cl(1b)	156.32(7)
C(1)–Ru–Cl(a)	117.68(9)	C(1)–Ru–Cl(1a)	121.83(8)
C(1)–Ru–Cl(b)	81.33(10)	C(1)–Ru–Cl(1b)	82.66(8)
P(1)–Ru–Cl(a)	87.15(5)	P(1)–Ru–Cl(1a)	88.31(5)
P(1)–Ru–Cl(b)	85.64(6)	P(1)–Ru–Cl(1b)	81.52(6)
P(2)–Ru–Cl(a)	89.49(5)	P(2)–Ru–Cl(1a)	86.46(5)
P(2)–Ru–Cl(b)	93.41(6)	P(2)–Ru–Cl(1b)	93.00(6)
Cl(a)–Ru–Cl(b)	36.62(8)	Cl(1a)–Ru–Cl(1b)	40.65(7)

[a] Both Cl(a) and Cl(b) have half occupancy.
[b] Both Cl(1a) and Cl(1b) have half occupancy.

Table 5
Cyclic voltammetric[a] data.

| Complex	$E_{1/2}$ (V) (ΔE_P (mV))[b]	
	Ru(III) → Ru(IV)	Ru(III) → Ru(II)
1	0.75 (100)	–
2	0.80 (150)	−0.67 (100)
3	0.77 (110)	−0.68 (80)
4	0.75 (150)	−0.70 (90)
5	0.80 (130)	−0.66 (90)

[a] In dichloromethane solution (298 K) at a scan rate of 50 mV s⁻¹.
[b] $E_{1/2} = (E_{pa} + E_{pc})/2$, where E_{pa} and E_{pc} are anodic and cathodic peak potentials, respectively; $\Delta E_p = E_{pa} - E_{pc}$.

for **5**) are deviated by a small amount from the ideal *trans* angle value of 180°. In each structure, the Ru–Cl bond lengths involving the two half occupancy Cl-atoms are very similar and within the range reported for the chloride coordinated ruthenium(III) complexes [17,26,28,29]. The Ru–P bond lengths are comparable with those reported for complexes of *trans*-{Ru(PPh₃)₂}³⁺ [11,17,26,28,29]. The Ru–C(ring), Ru–N(imine) and Ru–O(amide) bond lengths are very similar to the bond lengths observed in trivalent ruthenium complexes having the same coordinating atoms [11,17,28,29,31].

3.4. Electron transfer properties

The electron transfer properties of **1–5** have been examined in dimethylformamide with the help of cyclic voltammetry. The potential data are summarized in Table 5. Two representative cyclic voltammograms are depicted in Fig. 4. All the complexes display a quasi-reversible to irreversible Ru(III) → Ru(IV) oxidation in the potential range 0.75–0.80 V. In this oxidation response,
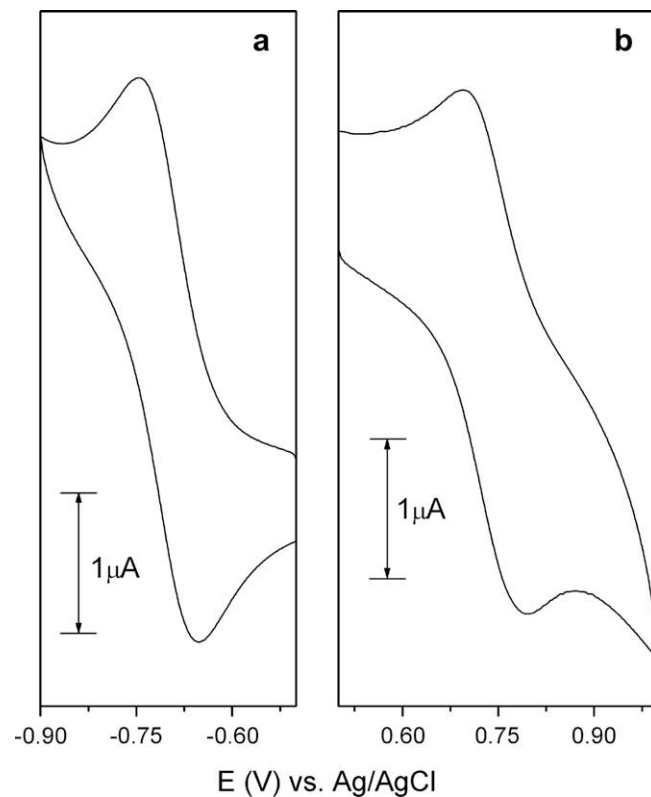
Fig. 4. Cyclic voltammograms (scan rate 50 mV s⁻¹): (a) reduction of *trans*-[Ru(apah4-H₃CO-C₆H₄)(PPh₃)₂Cl] (**4**) and (b) oxidation of *trans*-[Ru(apahCH₃)(PPh₃)₂Cl] (**1**) in dimethylformamide (0.1 M TBAP).

the cathodic peak current is significantly less than the anodic peak current particularly for complexes **2–5**. Barring complex **1** the remaining complexes also show a reversible Ru(III) → Ru(II) reduction within −0.66 to −0.70 V. The peak currents for the reduction response and the anodic peak current for the oxidation response are comparable with peak currents observed for known one-electron transfer processes under identical conditions [11–14,17,27–29]. In the cases of **2–5**, the potentials for both reduction and oxidation reflect a small but noticeable effect of the electronic nature of the substituent on the tridentate ligand (Table 5). For the most electron withdrawing substituent Cl (complex **5**) the potentials are highest and for the most electron releasing substituent OMe (complex **4**) the potentials are lowest. Satisfactory linear relationships are obtained when the potentials are plotted against the Hammett constants of the substituents [32]. Interestingly for our previously reported analogous complexes the Ru(III) → Ru(II) reduction response is not observed and except for the complex with acetylhydrazone the Ru(III) → Ru(IV) oxidation occurs at lower (by 350–400 mV) potentials [17]. At present we are not sure about the reasons for the differences in the electron transfer behavior and the oxidation potentials of the two analogous series of complexes which differ only in the type of substituent (R) present in the —CR=N— fragment of the tridentate ligand. Perhaps the change in the extent of distortions of the coordination geometry and hence in the electron energy levels due to the change of R from H to CH_3 plays some role in effecting the differences observed [33].

4. Conclusion

Synthesis and characterization of cyclometallated distorted octahedral ruthenium(III) complexes having the general molecular formula *trans*-[Ru(apahR)(PPh$_3$)$_2$Cl] with Schiff bases (H$_2$apahR) prepared from acid hydrazides and acetophenone have been described. The meridionally spanning dianionic ligand (L^{2-}) acts as C,N,O-donor in these complexes due to ruthenium mediated activation of *ortho*-C–H bond of the pendant phenyl group of H$_2$apahR. The molecular structures of two representative complexes have been determined by X-ray crystallography. The complexes are one-electron paramagnetic and display the characteristic rhombic EPR spectra in frozen solution commonly observed for distorted octahedral low-spin ruthenium(III) complexes. All the complexes are redox active and display a metal centred oxidation and except for one complex a metal centred reduction.

5. Supplementary material

CCDC 709287 and 709288 contain the supplementary crystallographic data for compounds *trans*-[Ru(apahCH$_3$)(PPh$_3$)$_2$Cl] (**1**) and *trans*-[Ru(apah4-Cl-C$_6$H$_4$)(PPh$_3$)$_2$Cl] (**5**), respectively. These data can be obtained free of charge from The Cambridge Crystallographic Data Centre via www.ccdc.cam.ac.uk/data_request/cif.

References

[1] G. Wilkinson, F.G.A. Stone, E.W. Abel (Eds.), Comprehensive Organometallic Chemistry, vol. 4, Pergamon, Oxford, 1982, p. 651.
[2] D.F. Schriver, M.I. Bruce (Eds.), Comprehensive Organometallic Chemistry II, vol. 7, Pergamon, Oxford, 1995, p. 291.
[3] V. Dragutan, I. Dragutan, L. Delaude, A. Demonceau, J. Organomet. Chem. 251 (2007) 765.
[4] A.J. Hewitt, J.H. Holloway, R.D. Peacock, J.B. Raynor, I.L. Wilson, J. Chem. Soc. Dalton Trans. (1976) 579.
[5] L.H. Pignolet, S.H. Wheeler, Inorg. Chem. 19 (1980) 935.
[6] M.M. Taqui Khan, D. Srinivas, R.I. Kureshy, N.H. Khan, Inorg. Chem. 29 (1990) 2320.
[7] M. Ke, S.J. Rettig, B.R. James, D. Dolphin, J. Chem. Soc. Chem. Commun. (1987) 1110.
[8] J.W. Seyler, C.R. Leidner, Inorg. Chem. 29 (1990) 3636.
[9] M. Ke, C. Sishta, B.R. James, D. Dolphin, J.W. Sparapany, J.A. Ibers, Inorg. Chem. 30 (1991) 4766.
[10] M. Beley, J.P. Collin, R. Louis, B. Metz, J.P. Sauvage, J. Am. Chem. Soc. 113 (1991) 8521.
[11] G.K. Lahiri, S. Bhattacharya, M. Mukherjee, A.K. Mukherjee, A. Chakravorty, Inorg. Chem. 26 (1987) 3359.
[12] P. Ghosh, A. Pramanik, N. Bag, G.K. Lahiri, A. Chakravorty, J. Organomet. Chem. 454 (1993) 237.
[13] R. Hariram, B.K. Santra, G.K. Lahiri, J. Organomet. Chem. 540 (1997) 155.
[14] P. Munshi, R. Samanta, G.K. Lahiri, J. Organomet. Chem. 586 (1999) 176.
[15] S. Das, S. Pal, J. Organomet. Chem. 689 (2004) 352.
[16] S. Das, S. Pal, J. Organomet. Chem. 691 (2006) 2575.
[17] R. Raveendran, S. Pal, J. Organomet. Chem. 692 (2007) 824.
[18] T.A. Stephenson, G. Wilkinson, J. Inorg. Nucl. Chem. 28 (1966) 945.
[19] W.E. Hatfield, in: E.A. Boudreaux, L.N. Mulay (Eds.), Theory and Applications of Molecular Paramagnetism, Wiley, New York, 1976, p. 491.
[20] SMART version 5.630 and SAINT-plus version 6.45, Bruker-Nonius Analytical X-ray Systems Inc., Madison, WI, USA, 2003.
[21] G.M. Sheldrick, SADABS, Program for Area Detector Absorption Correction, University of Göttingen, Göttingen, Germany, 1997.
[22] G.M. Sheldrick, SHELX-97 Structure Determination Software, University of Göttingen, Göttingen, Germany, 1997.
[23] P. McArdle, J. Appl. Crystallogr. 28 (1995) 65.
[24] W. Kemp, in: Organic Spectroscopy, Macmillan, Hampshire, 1987, pp. 62–65.
[25] K. Nakamoto, in: Infrared and Raman Spectra of Inorganic and Coordination Compounds, Wiley, New York, 1986, pp. 241–244.
[26] F. Basuli, A.K. Das, G. Mostafa, S.M. Peng, S. Bhattacharya, Polyhedron 19 (2000) 1663.
[27] R. Raveendran, S. Pal, Polyhedron 24 (2005) 57.
[28] R. Raveendran, S. Pal, Inorg. Chim. Acta 359 (2006) 3212.
[29] R. Raveendran, S. Pal, Polyhedron 27 (2008) 655.
[30] S. Bhattacharya, A. Chakravorty, Proc. Indian Acad. Sci. (Chem. Sci.) 95 (1985) 159.
[31] S.N. Pal, S. Pal, Eur. J. Inorg. Chem. (2003) 4244.
[32] J. March, in: Advanced Organic Chemistry, 4th ed., Wiley, New York, 1992, p. 280.
[33] P. Basu, S.B. Choudhury, S. Pal, A. Chakravorty, Inorg. Chem. 28 (1989) 2680.